Theoretical Study on the Molecular Mechanism of the Domino Cycloadditions between Dimethyl Acetylenedicarboxylate and Naphthaleno- and Anthracenofuranophane

Luis R. Domingo,* M. Teresa Picher, Juan Andrés,† and Mónica Oliva†

Departamento de Química Orgánica, Universidad de Valencia, Dr. Moliner 50, 46100 Burjassot, Valencia, Spain, and Departament de Ciències Experimentals, Universitat Jaume I, Apartat 224, 12080 Castelló, Spain

Received July 23, 1998

AM1, B3LYP/6-31G*//AM1, and B3LYP/6-31G* computational studies were performed to select the reaction pathway controlling the reactions between dimethyl acetylenedicarboxylate (DMAD) and two furanophanes, naphthalenofuranophane and anthracenofuranophane. For these domino reactions, several pathways have been characterized on the potential energy surface corresponding to two consecutive cycloadditions. The first step corresponds to a [4 + 2] intermolecular cycloaddition of DMAD with the furan ring or with the naphthalene or anthracene ring of both furanophane systems to yield an oxabicyclo[2.2.1]heptadiene or a bicyclo[2.2.2]octadiene intermediate, respectively. The second step corresponds to [4 + 2] intramolecular cycloadditions of these intermediates. For the naphthalenofuranophane, the most favorable reaction pathway takes place along the initial [4 + 2] intermolecular cycloaddition involving the nonsubstituted ring of the naphthalene system to give a benzobicyclo[2.2.2]octadiene intermediate, which by a [4 + 2] intramolecular cycloaddition between the substituted double bond of this intermediate and the furan ring affords the final cycloadduct. For the anthracenofuranophane, the most favorable reaction pathway takes place along the initial [4 + 2] intermolecular cycloaddition involving the furan ring to give an oxabicyclo[2.2.1]-heptadiene intermediate, which by a [4 + 2] intramolecular cycloaddition between the nonsubtituted double bond of the bicyclic system and the naphthalene system affords the final cycloadduct. An analysis of energetic contributions to the potential energy barriers identifies the different factors controlling the competitive reaction pathways. The present theoretical results are able to explain the available experimental data.

Introduction

Diels−Alder rearrangements are by themselves extremely useful transformations in organic chemistry. However, by combining two or more cycloadditions of this type, the effects can be multiplied. This type of domino reaction is synthetically valuable and provides mechanistically intriguing rearrangements involving two or more bond-forming processes which take place under the same reaction conditions, without adding additional reagents and catalysts and in which the subsequent reactions result as a consequence of the functionality formed in the previous step.[1−4]

Our research program has long maintained an interest in this kind of chemical reaction, and the understanding of the characteristic feature of these consecutive cycloadditions prompted us to explore further the mechanistic aspects. In previous theoretical works, the domino cycloaddition reactions between acetylene derivatives as dienophiles and bicyclopentadiene[5] and *N*,*N*′-dipyrrolylmethane[6,7] as diene systems have been studied. Therefore, it seemed of interest to extend these studies to domino reactions containing furan rings, which have not been treated by computational methods and for which no generally accepted molecular mechanism has emerged. In particular, the domino reactions between dimethyl acetylenedicarboxylate (DMAD, **1**) and two cyclophanes containing a furan ring, reported independently by Wasserman and Kitzing[8] and Wynberg and Helder,[9] can be considered important examples of the utility of this methodology for the synthesis of complex polycyclic systems.

In the present paper, the following reactions have been studied as computational models of this kind of domino cycloaddition: the reaction between **1** and [2,2](1,4)-naphthaleno(2,5)furanophane[8] (**2**) and the reaction between **1** and [2,2](9,10)anthraceno(2,5)furanophane[9] (**3**). Our aim was to characterize the reaction pathways of the above domino reactions. The analysis of the potential energy surface (PES) and the location of transition structures (TSs) and related minima provide knowledge regarding the nature of the molecular mechanism and allow us to rationalize and explain the experimental observations.

Computational Methods

The PESs of the two domino cycloadditions have been calculated in detail to ensure that all relevant stationary points

† Universitat Jaume I.

(1) Ho, T. L. *Tandem Organic Reaction*; Wiley: New York, 1992.
(2) Tietze, L. F.; Beifuss, U. *Angew. Chem., Int. Ed. Engl.* **1993**, *32*, 131.
(3) Tietze, L. F. *Chem. Rev.* **1996**, *96*, 115.
(4) Winkler, J. D. *Chem. Rev.* **1996**, *96*, 167.
(5) Domingo, L. R.; Arnó, M.; Andrés, J. *Tetrahedron Lett.* **1996**, *37*, 7573.
(6) Domingo, L. R.; Arnó, M.; Andrés, J. *J. Am. Chem. Soc.* **1998**, *120*, 1617.
(7) Domingo, L. R.; Picher, M. T.; Arnó, M.; Andrés, J.; Safont, V. S. *THEOCHEM* **1998**, *426*, 257.
(8) Wasserman, H. H.; Kitzing, R. *Tetrahedron Lett.* **1969**, 3343.
(9) Wynberg, H.; Helder, R. *Tetrahedron Lett.* **1971**, 4317.

10.1021/jo981442k CCC: $18.00
Published on Web 04/10/1999

Scheme 1

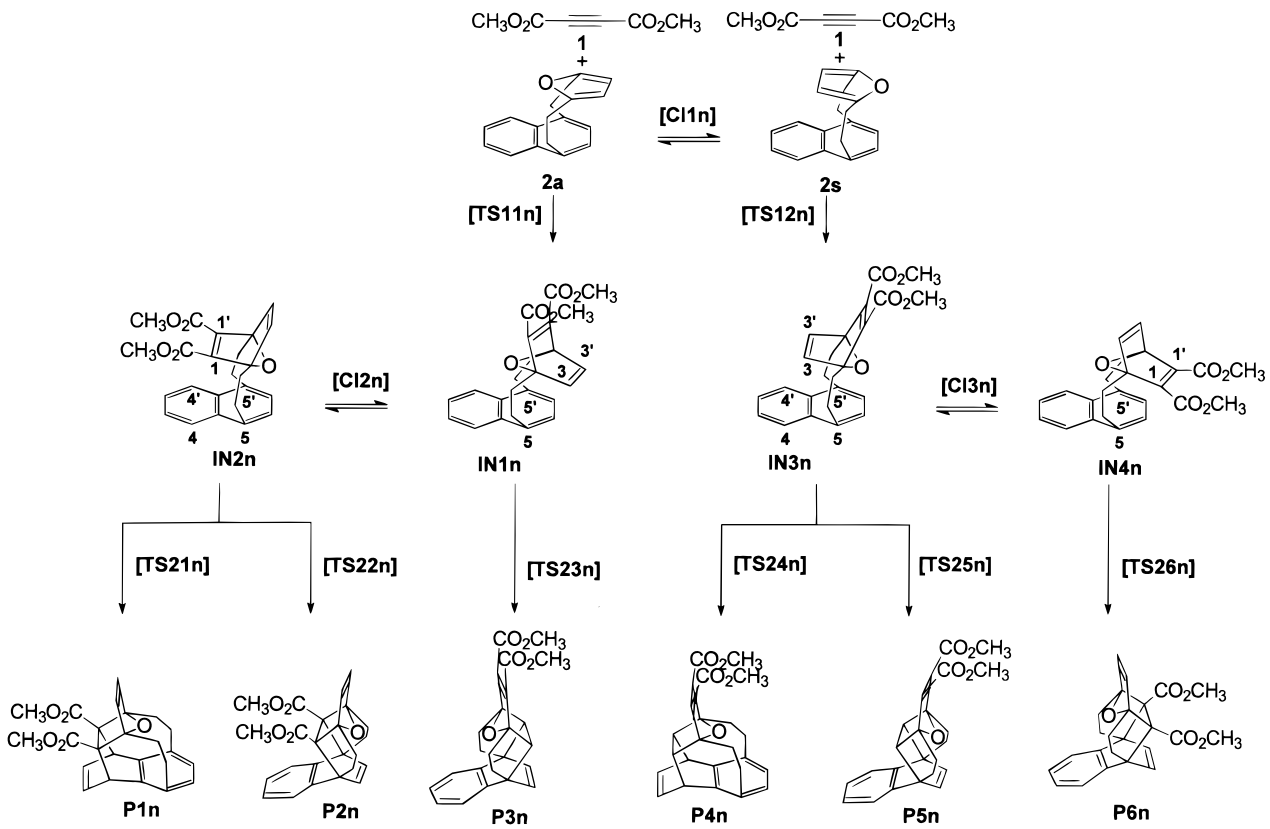

Mode A

have been located and properly characterized. All molecular geometries have been fully optimized using the semiempirical AM1 methods[10] implemented in the MOPAC93 package programs.[11]

The stationary points along the PES have been located without any geometrical restriction and have been characterized through the calculation of the force constants matrix by ensuring that they correspond to minima or saddle points, i.e., they have zero or one and only one imaginary frequency, respectively. Several conformational structures related to the rotation of the carboxylate groups have been considered, and the most stable ones have been chosen. Optimized geometries of all structures are available from the authors.

AM1, in common with other semiempirical methods, has acknowledged weakness, for example, in dealing with absolute values of activation energies. Moreover, the large size of the present molecular systems dissuades the use of high level ab initio methods to obtain accurate energies. Recently, Jursic et al.[12−16] and Oliva et al.[17] have shown that the B3LYP/6-31G*//AM1 approach renders qualitatively correct results in studies of related Diels−Alder reactions, and subsequently this computational strategy can be applied in the study of large organic molecules.[12−17] Consequently, we have used the hybrid B3LYP method, consisting of the gradient-corrected functionals of Becke,[18] and Lee, Yang, and Parr[19] for exchange and nonlocal correlation, respectively, and the 6-31G* basis set[20] to calculate energetic parameters with the AM1 optimized geometries. Finally, the more relevant stationary points along reaction pathways for system **1** + **2** have been fully optimized at the B3LYP/6-31G* level to check the reliability of this strategy. DFT calculations have been done using the Gaussian 94 program.[21]

Results

For these domino reactions, two initial [4 + 2] intermolecular cycloadditions are possible: (i) mode A, in which DMAD is added to the furan ring and (ii) mode B, in which DMAD is added to the naphthalene or anthracene rings of both furanophanes.

(a) Domino Reaction between 1 and 2. In Schemes 1 (mode A) and 2 (mode B), the stationary points corresponding to the domino reaction between **1** and **2** have been presented together with the atom numbering, and the geometries of the TSs corresponding to the chemical conversion along the different reaction pathways are depicted in Figures 1 (mode A) and 2 (mode B). The relative energies are summarized in Table 1.

For the furanophane **2**, two conformations are possible: anti, **2a**, and syn, **2s**, the former being 4.1 kcal mol^{-1} more stable. B3LYP/6-31G*//AM1 energetic data are given through the text. An unfavorable interaction

(10) Dewar, M. J. S.; Zoebisch, E. G.; Healy, E. F.; Stewart, J. J. P. *J. Am. Chem. Soc.* **1985**, *107*, 3902.
(11) Stewart, J. J. P. Fujitsu Corp. Ltd.: Tokyo, 1993.
(12) Jursic, B. S. *THEOCHEM* **1995**, *358*, 139.
(13) Jursic, B. S. *THEOCHEM* **1996**, *365*, 55.
(14) Jursic, B. S. *THEOCHEM* **1996**, *379*, 85.
(15) Jursic, B. S.; LeBlanc, B. *J. Heterocycl. Chem.* **1996**, 1389.
(16) Jursic, B. S. *THEOCHEM* **1998**, *423*, 189.
(17) Sbai, A.; Branchadell, V.; Ortuño, R. M.; Oliva, A. *J. Org. Chem.* **1997**, *62*, 3049.
(18) Becke, A. D. *J. Chem. Phys.* **1993**, *98*, 5648.
(19) Lee, C.; Yang, W.; Parr, R. G. *Phys. Rev. B* **1988**, *37*, 785.
(20) Hehre, W. J.; Radom, L.; Schleyer, P. v. R.; Pople, J. A. *Ab initio Molecular Orbital Theory*; Wiley: New York, 1986.
(21) Frisch, M. J.; Trucks, G. W.; Schlegel, H. B.; Gill, P. M. W.; Johnson, B. G.; Robb, M. A.; Cheeseman, J. R.; Keith, T.; Petersson, G. A.; Montgomery, J. A.; Raghavachari, K.; Al-Laham, M. A.; Zakrzewski, V. G.; Ortiz, J. V.; Foresman, J. B.; Cioslowski, J.; Stefanov, B. B.; Nanayakkara, A.; Challacombe, M.; Peng, C. Y.; Ayala, P. Y.; Chen, W.; Wong, M. W.; Andres, J. L.; Replogle, E. S.; Gomperts, R.; Martin, R. L.; Fox, D. J.; Binkley, J. S.; Defrees, D. J.; Baker, J.; Stewart, J. P.; Head-Gordon, M.; Gonzalez, C.; Pople, J. A. Gaussian, Inc.: Pittsburgh, PA, 1995.

Scheme 2

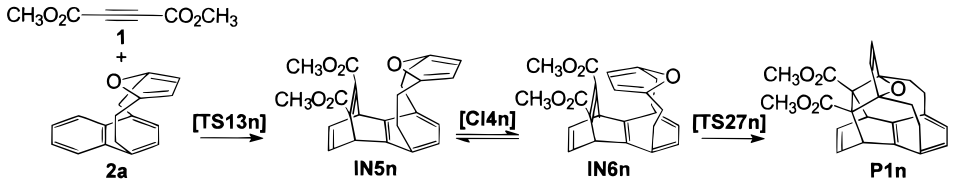

Mode B

Table 1. Relative Energies (kcal mol^{-1}) of Transition Structures, Intermediates, and Products with Respect to Reactants for the Domino Reaction between 1 and 2[a]

	$\Delta E1$[b]	$\Delta E2$[c]	$\Delta E3$[d]
1 + 2a	0.0	0.0	0.0
1 + 2s	0.6	4.1	3.5
TS11n	39.2	24.9 (24.9)	17.5 (17.5)
TS12n	39.0	29.0 (24.9)	20.6 (17.1)
TS13n	40.8	31.4 (31.4)	24.8 (24.8)
IN1n	3.6	1.6	−5.4
IN2n	6.1	8.0	0.4
IN3n	3.8	6.4	−1.7
IN4n	4.0	0.6	
IN5n	−20.5	−16.2	
IN6n	−29.7	−12.2	
CI1n	8.7	18.8	17.2
CI2n	9.7	18.5	12.0
CI3n	9.4	18.7	
CI4n	−11.4	4.5	
TS21n	49.9	34.4 (26.4)	27.3 (26.9)
TS22n	68.7	66.8 (58.8)	
TS23n	51.6	43.8 (42.2)	
TS24n	42.9	31.6 (25.2)	25.7 (27.4)
TS25n	44.0	35.3 (28.9)	
TS26n	62.5	50.2 (49.6)	
TS27n	36.8	29.2 (41.4)	
P1n	6.8	5.8	−0.1
P2n	22.2	16.5	
P3n	11.1	4.1	
P4n	−7.6	−4.6	−11.2
P5n	0.9	−2.6	
P6n	30.5	19.3	

[a] Values were obtained at AM1 ($\Delta E1$), B3LYP/6-31G*//AM1 ($\Delta E2$), and B3LYP/6-31G* ($\Delta E3$) levels. Values in parentheses correspond to PEB. [b] AM1 heat of formation of **1** + **2a** is −47.3 kcal mol^{-1}. [c] B3LYP/6-31G*//AM1 total energy of **1** + **2a** is −1303.794 489 au. [d] B3LYP/6-31G* total energy of **1** + **2a** is −1303.811 485 au.

between the π aromatic systems of both the furan and the naphthalene moiety in the syn conformation is responsible for the larger energy for **2s** relative to **2a**. This result agrees with ^{1}H NMR data of **2** reported by Wasserman and Keehn.[22]

The domino reaction between **1** and **2** can takes place along seven reaction pathways (six for mode A and one for mode B) which involve two consecutive cycloadditions. For the domino reactions along mode A (Scheme 1), the first step is a [4 + 2] intermolecular cycloaddition of the acetylenic fragment of **1** to the less hindered face of the furan ring in the anti and syn conformations of **2** to give two oxabicyclo[2.2.1]heptadiene intermediates, **IN1n** and **IN3n**, via two diastereomeric TSs, **TS11n** and **TS12n**, respectively (see Figure 1). The main difference between both TSs is the arrangement of the furan ring involved in the intermolecular cycloaddition relative to the naphthalene system. Both TSs are associated with identical potential energy barriers (PEBs), 24.9 kcal mol^{-1}, **TS11n** being more stable than **TS12n** as a result of the larger

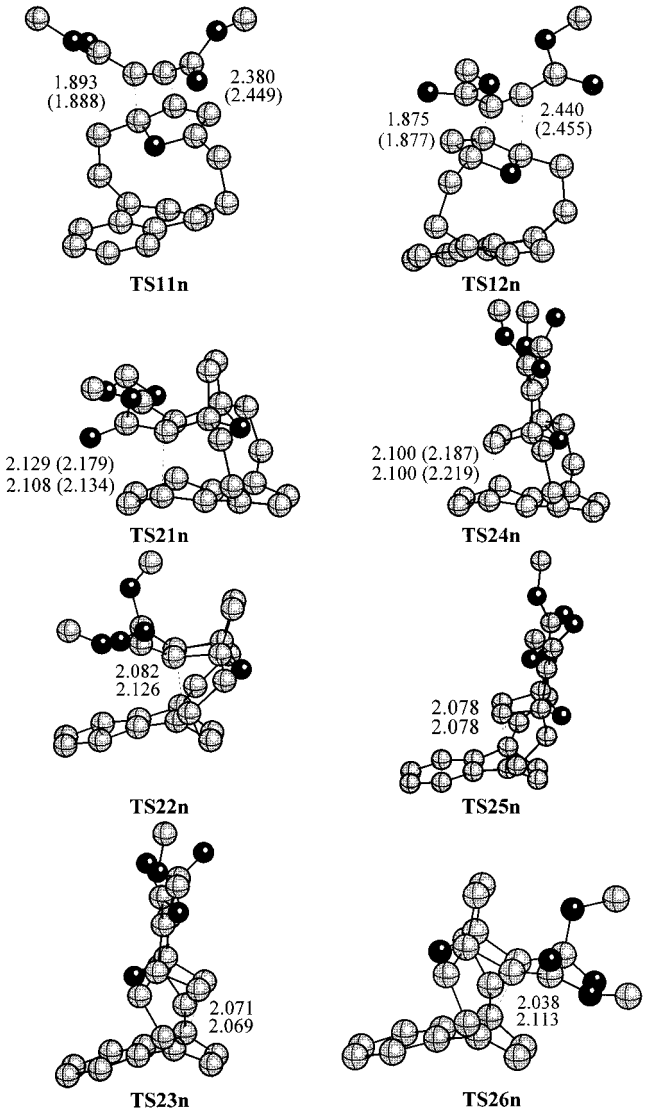

Figure 1. Transition stuctures corresponding to mode A of the domino cycloaddition reaction between **1** and **2**. The values of the lengths of the C−C bonds directly involved in the cycloaddition obtained at AM1 and B3LYP/6-31G* (in parentheses) are given in angstroms.

stability of **2a** in comparison with **2s**. The conformers **2a** and **2s** can be interconverted by rotation of the two carbon chains connecting the furan and naphthalene systems via a confomational interconversion, **CI1n**. A similar interconversion takes place for the intermediates **IN1n** and **IN3n**, which by means of a conformational interconversion can give **IN2n** and **IN4n**, via **CI2n** and **CI3n**, respectively. The energies associated with these conformational interconversions (in the range of 18.5−18.7 kcal mol^{-1}) are lower than those corresponding to the PEBs of first or second cycloadditions.

(22) Wasserman, H. H.; Keehn, P. M. *Tetrahedron Lett.* **1969**, 3227.

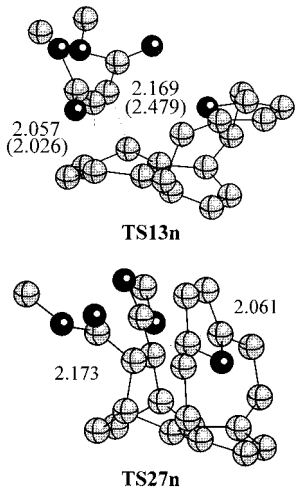

Figure 2. Transition stuctures corresponding to mode B of the domino cycloaddition reaction between **1** and **2**. The values of the lengths of the C−C bonds directly involved in the cycloaddition obtained at AM1 and B3LYP/6-31G* (in parentheses) are given in angstroms.

Several modes of intramolecular cyclizations are possible in the second stage along mode A as a result of the presence of several reactive sites in these intermediates: positions 1,1′ and 3,3′ belonging to the substituted and nonsubstituted double bonds of the oxabicyclo[2.2.1]-heptadiene system (dienophile residue), positions 4,4′ and 5,5′ belonging to the naphthalene system (diene residue), and the two possible attacks to the positions 5,5′ (endo and exo correspond to the attack over and outside of the naphthalene system, respectively). Thus, the intermediates formed in the initial step can render six final cycloadducts via six TSs related to different types of [4 + 2] intramolecular cycloadditions. From **IN1n**, only the cycloadduct **P3n** can be obtained via **TS23n** (42.2 kcal mol^{-1}), whereas **P1n** and **P2n** can be obtained from **IN2n** via **TS21n** (26.4 kcal mol^{-1}) and **TS22n** (58.8 kcal mol^{-1}), respectively. The cycloadducts **P4n** and **P5n** can be obtained from **IN3n** via **TS24n** (25.2 kcal mol^{-1}) and **TS25n** (28.9 kcal mol^{-1}), respectively, and **P6n** can be obtained from **IN4n** via **TS26n** (49.6 kcal mol^{-1}). Values in parentheses correspond to PEBs.

TS21n, **TS22n**, and **TS26n** are associated with the intramolecular attack of the substituted double bond of the dienophile fragment, positions 1,1′, to the positions 4,4′, 5,5′ (endo attack), and 5,5′ (exo attack) of the naphthalene system, respectively. **TS23n**, **TS24n**, and **TS25n** are associated with the intramolecular attack of the nonsubstituted double bond of the dienophile fragment, positions 3,3′, to the positions 5,5′ (exo attack), 4,4′, and 5,5′ (endo attack) of the naphthalene system, respectively.

For the domino reaction along mode B (Scheme 2), the first step is a [4 + 2] intermolecular cycloaddition of the acetylenic fragment of **1** to the 4,4′ positions of the naphthalene system in the anti conformation **2a** to give the benzobicyclo[2.2.2]octadiene intermediate **IN5n**, via **TS13n**. The PEB associated with this process is 31.4 kcal mol^{-1}. The intermediate **IN5n** can be interconverted into the intermediate **IN6n** via a conformational interconversion along **CI4n** (20.7 kcal mol^{-1}). The second step is a [4 + 2] intramolecular cycloaddition reaction of the intermediate **IN6n**, associated with the attack of the substituted double bond (positions 1,1′) to the positions 2,2′ of the furan ring, to yield the final cycloadduct **P1n**, via **TS27n** (41.4 kcal mol^{-1}).

(b) Domino Reaction between 1 and 3. In Schemes 3 (mode A) and 4 (mode B), the stationary points corresponding to the domino reaction between **1** and **3** have been presented together with the atom numbering,

Scheme 3

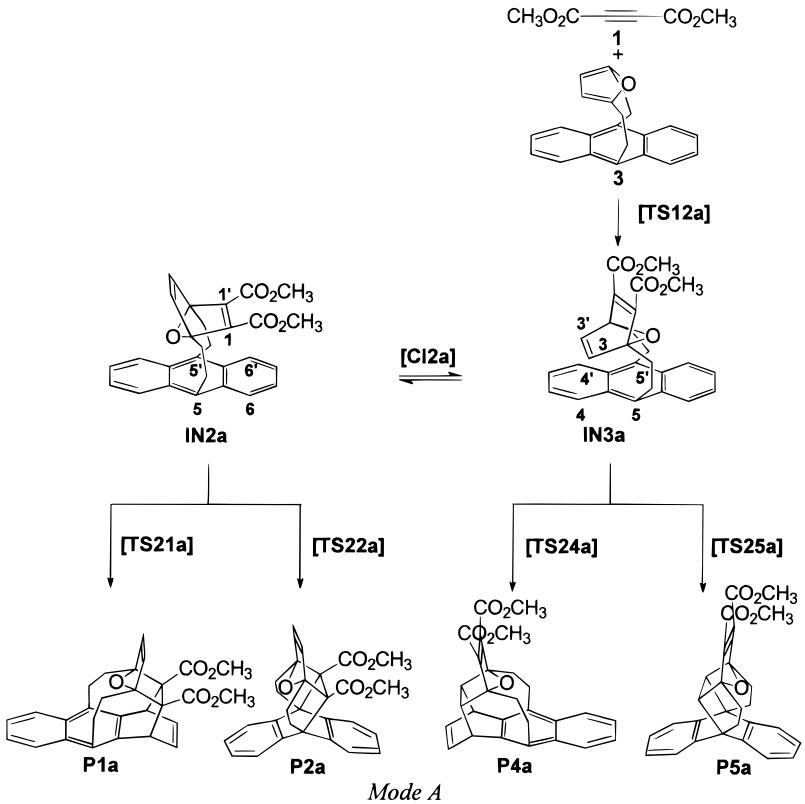

Scheme 4

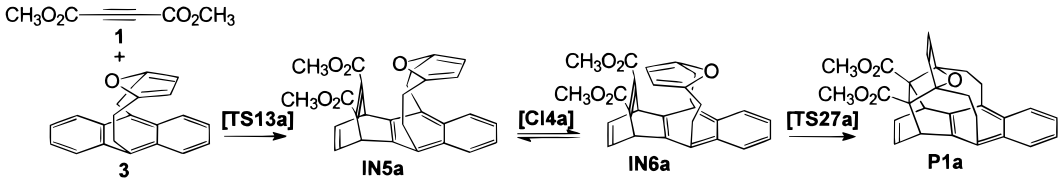

Mode B

Table 2. Relative Energies (kcal mol^{-1}) of Transition Structures, Intermediates, and Products with Respect to Reactants for the Domino Reaction between 1 and 3[a]

	$\Delta E1$[b]	$\Delta E2$[c]	$\Delta E3$[d]
1 + 3	0.0	0.0	0.0
TS12a	38.7	24.2 (24.2)	
TS13a	39.6	29.1 (29.1)	22.4
IN3a	2.3	−2.9	
IN2a	3.5	−2.4	
IN5a	−26.1	−22.7	
IN6a	−25.4	−23.0	
CI2a	−13.1	8.8	
CI4a	−17.7	−6.2	
TS21a	46.2	28.6 (31.0)	
TS22a	64.6	55.6 (58.0)	
TS24a	39.4	26.0 (28.9)	19.7
TS25a	39.7	24.9 (27.8)	24.7
TS27a	29.3	21.0 (44.0)	
P1a	0.2	−0.8	
P2a	14.6	−3.0	
P4a	−15.9	−15.3	
P5a	−8.4	−23.1	

[a] Values were obtained at AM1 ($\Delta E1$), B3LYP/6-31G*//AM1 ($\Delta E2$), and B3LYP/6-31G* ($\Delta E3$) levels. Values in parentheses correspond to PEB. [b] AM1 heat of formation of **1** + **3** is −21.9 kcal mol^{-1}. [c] B3LYP/6-31G*//AM1 total energy of **1** + **3** is −1457.423 143 au. [d] B3LYP/6-31G* total energy of **1** + **3** is −1457.440 382 au.

and the geometries of the TSs corresponding to the chemical conversion along the different reaction pathways are depicted in Figures 3 (mode A) and 4 (mode B). The relative energies are summarized in Table 2. For sake of clarity, a notation similar to that of previous reaction pathways has been selected for the stationary points of this domino reaction.

The domino reaction between **1** and **3** can take place along five reaction pathways (four for mode A and one for mode B) which involve two consecutive Diels−Alder cycloadditions. For the domino reactions along mode A, the first and common step is a [4 + 2] intermolecular cycloaddition of the acetylenic fragment of **1** to the less hindered face of furan ring of **3** to give an oxabicyclo-[2.2.1]heptadiene intermediate, **IN3a**, via the **TS12a**, with a PEB of 24.2 kcal mol^{-1}. The intermediate **IN3a** can be interconverted into the intermediate **IN2a** via a conformational interconversion along **CI2a** (17.1 kcal mol^{-1}). The second steps along mode A take place along four [4 + 2] intramolecular cycloaddition reactions of these intermediates to yield the final cycloadducts **P4a** and **P5a** from **IN3a** and **P1a** and **P2a** from **IN2a**, via the TSs **TS24a** (28.9 kcal mol^{-1}), **TS25a** (27.8 kcal mol^{-1}), **TS21a** (31.0 kcal mol^{-1}), and **TS22a** (58.0 kcal mol^{-1}), respectively. **TS24a** and **TS25a** are associated with the intramolecular attack of the nonsubstituted double bond of the oxabicyclo[2.2.1]heptadiene system of **IN3a**, positions 3,3′, to the 4,4′ or 5,5′ positions of the anthracene system, respectively. **TS21a** and **TS22a** correspond to the intramolecular attack of the substituted double bond of the oxabicyclo[2.2.1]heptadiene system of **IN2a**, positions

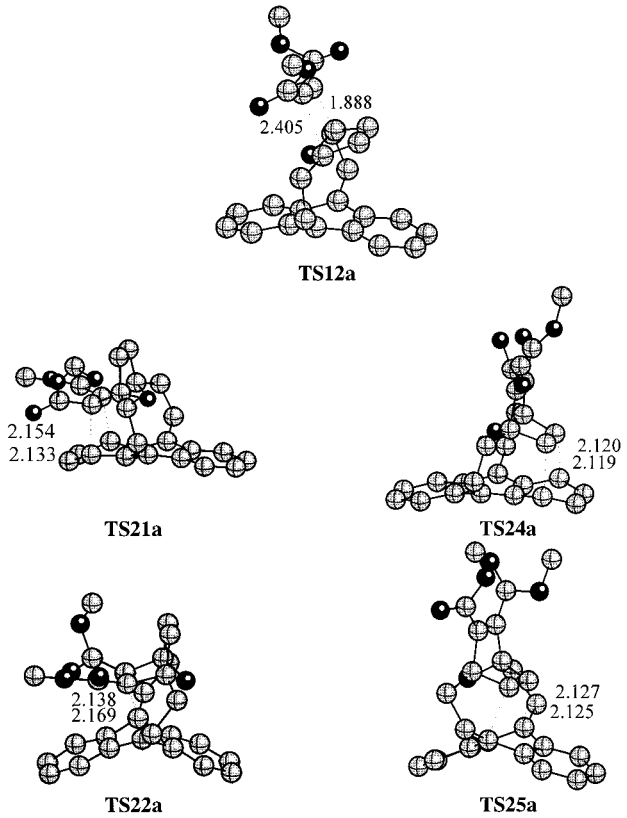

Figure 3. Transition structures corresponding to mode A of the domino cycloaddition reaction between **1** and **3**. The values of the lengths of the C−C bonds directly involved in the cycloaddition obtained at AM1 are given in angstroms.

1,1′, to the 6,6′ or 5,5′ positions of the anthracene system, respectively.

For the domino reaction along mode B, the first step is a [4 + 2] intermolecular cycloaddition of the acetylenic fragment of **1** to the 4,4′ positions of the anthracene system to give the naphthobicyclo[2.2.2]octadiene intermediate **IN5a**, via **TS13a**, with a PEB associated with this process of 29.1 kcal mol^{-1}. The intermediate **IN5a** can be interconverted into the intermediate **IN6a** via a conformational interconversion along **CI4a** (17.1 kcal mol^{-1}). The second step is a [4 + 2] intramolecular cycloaddition reaction of the intermediate **IN6a**, associated with the attack of the substituted double bond (positions 1,1′) to the positions 2,2′ of the furan ring, to yield the final cycloadduct **P1a**, via **TS27a** (44.0 kcal mol^{-1}).

Discussion

An analysis of the geometries of the TSs corresponding to the [4 + 2] intermolecular cycloadditions along mode A for the two furanophane systems, **TS11n**, **TS12n**, and **TS12a**, shows that the two carboxylate groups of the

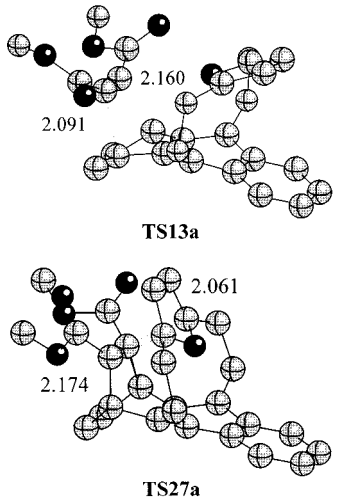

Figure 4. Transition stuctures corresponding to mode B of the domino cycloaddition reaction between **1** and **3**. The values of the lengths of the C−C bonds directly involved in the cycloaddition obtained at AM1 are given in angstroms.

dienophile system are located on perpendicular planes. This arrangement has the following effects: (i) it allows a favorable π-delocalization along both carboxylate groups, (ii) it increases the electron-withdrawing ability of these groups and (iii) it increases the asynchronicity of the cycloaddition process, the lengths of the two C−C forming bonds being around 1.9 and 2.4 Å. A similar behavior has been found for related cycloadditions.[23−25] The absence of these effects in the TSs corresponding to the [4 + 2] intramolecular cycloadditions renders similar values for the two C−C bonds being formed (in the range 2.0−2.1 Å), promoting symmetric TSs. In addition, the presence of the two carboxylate substituents on the dienophile fragment does not substantially modify the geometrical parameters in the second stage.

For the first step of the domino reactions along mode A, B3LYP/6-31G*//AM1 calculations render similar PEBs: 24.9 (**TS11n**), 24.9 (**TS12n**), and 24.2 (**TS12a**) kcal mol^{-1}. Therefore, the PEBs of these [4 + 2] intermolecular cycloadditions are not dependent on the type of fused rings (naphthalene or anthracene). Moreover, the values of the PEBs for the first step of the domino reactions along mode B, 31.4 (**TS13n**) and 29.1 (**TS13a**) kcal mol^{-1}, are larger than those for mode A. These results can be related to the loss of the aromatic character of theses systems along these cycloaddition processes; the fused rings have more aromatic character than the furan ring.

An analysis of the energetic results presented in Tables 1 and 2 shows that for the reaction pathways corresponding to mode A, the second and [4 + 2] intramolecular cyloaddition renders the TSs with higher relative energies, whereas for mode B, the TS associated with first step corresponding with the [4 + 2] intermolecular cycloaddition is the most energetic.

These energetic results can be used also to understand the relative energies for the TSs associated with the second step along mode A. These relative energies can be decomposed into three contributions: (i) The first one is associated with the participation of the substituted double bond of the dienophile fragment in the intramolecular cycloaddition (attack of the positions 1,1′ relative to 3,3′). The electron-withdrawing ability of the $-COOCH_3$ groups activates the substituted double bond along the cycloaddition process, relative to the nonsubstituted double bond.[5−7] (ii) The second factor appears as a differential strain along the intramolecular attack of the double bonds of the oxabicyclo[2.2.1]heptadiene fragment to 5,5′ positions (formation of five-membered rings) or to 4,4′ (6,6′) positions (formation of seven-membered rings) of the naphthalene or anthracene systems, which is less favorable for the five-membered ring formation (iii). The third factor is associated with an unfavorable interaction that appears between the carboxylate groups of the dienophile fragment and the π aromatic system of both naphthalene or anthracene systems along the intramolecular attack of the substituted double bond, which is higher for the attack to 5,5′ positions than to 4,4′ positions.

The energetic results given in Table 1 for **1** + **2** show that the most favorable reaction pathway for mode A is associated with the formation of the final cycloadduct **P4n**. The second step of this pathway corresponds to the intramolecular attack of the nonsubstituted double bond of the oxabicyclo[2.2.1]heptadiene system to the nonsubstituted ring of the naphthalene system of the intermediate **IN3n**, via **TS24n**. The unfavorable interactions that appear between the carboxylate groups and the naphthalene system in **TS21n** penalize the formation of **P1n** cycloadduct. This fact is in contrast to related domino cycloadditions in which the isomers resulting from the activated double bond attack are favored.[5−7]

For the reaction pathway of mode B, formation of the final cycloadduct **P1n**, the first step that corresponds to the intermolecular attack of the acetylenic fragment of **1** to the nonsubstituted ring of the naphthalene system, via **TS13n**, is sligthly more favorable (0.4 kcal mol^{-1}) than the formation of the cycloadduct **P4n** along mode A. In consequence, for **1** + **2**, the final cycloadduct **P1n** is preferentially formed.

To check the B3LYP/6-31G*//AM1 approach, the most relevant stationary points along the formation of the final cycloadducts **P1n** and **P4n** have been fully optimized at the B3LYP/6-31G* level (see Table 1). The PEBs for the [4 + 2] intermolecular cycloadditions decrease in the range of 6.6−7.8 kcal mol^{-1} relative to B3LYP/6-31G*//AM1 calculations. Thus, the PEB associated with **TS12n** (17.1 kcal mol^{-1}) at B3LYP/6-31G* level is similar to values for related [4 + 2] intermolecular cycloadditions studied by us.[25] The difference in energy between **TS13n** (mode B) and **TS24n** (mode A) increases up to 0.9 kcal mol^{-1}. The theoretical results used to explain the experimental data prevail at this higher calculation level and allow us to explain the formation of the final cycloadduct **P1n**. In addition, an analysis of the geometrical parameters of these TSs shows that the geometries are not dependent on calculation level (see Figure 1), except for **TS13n** corresponding to the first step of mode B, for which the B3LYP/6-31G* method gives an asynchronous process (2.0 and 2.5 Å) instead of the synchronous character given by AM1 results (2.1 and 2.2 Å).

The energetic results given in Table 2 for **1** + **3** show that the most favorable reaction pathway for mode A is

(23) Domingo, L. R.; Jones, R. A.; Picher, M. T.; Sepúlveda-Arqués, J. *Tetrahedron* **1995**, *51*, 8739.
(24) Domingo, L. R.; Picher, M. T.; Andrés, J.; Moliner, V.; Safont, V. S. *Tetrahedron* **1996**, *52*, 10693.
(25) Domingo, L. R.; Picher, M. T.; Zaragozá, R. J. *J. Org. Chem.* **1998**, *63*, 9183.

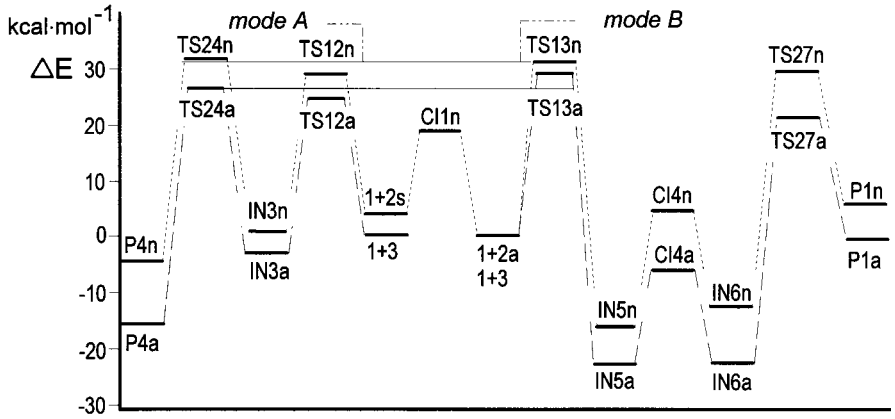

Figure 5. Energy profiles of the more favorable reaction pathways along modes A and B for the domino reactions between **1** and **2**, dotted lines, and **1** and **3**, dashed lines.

associated with the intermolecular attack of **1** to the furan ring of **3**, along **TS12a**, and a subsequent ring closure process involving the nonsubstituted double bond of oxabicyclo[2.2.1]heptadiene intermediate **IN3a** with formation of the **P4a** and **P5a** cycloadducts, via **TS24a** and **TS25a**, respectively. Although AM1 calculations demonstrated **TS24a** to be 0.3 kcal mol^{-1} less energetic than **TS25a**, B3LYP/6-31G*//AM1 calculations showed the latter to be 1.1 kcal mol^{-1} more stable. A full B3LYP/6-31G* optimization for these TSs shows **TS24a** to be 5.0 kcal mol^{-1} more stable than **TS25a**, and consequently the formation of the final cycloadduct **P4a** is clearly favored. This result can be explained by the more favorable seven-membered ring formation along the intramolecular cycloaddition involving the nonsubstituted double bond of the oxabicycloheptadiene system.

The energy associated with **TS13a** (first step along mode B) is 3.1 kcal mol^{-1} higher than that for **TS24a** (second step along mode A). This fact justifies the formation of the final cycloadduct **P4a**. These theoretical results prevail at the full B3LYP/6-31G* calculation level, with **TS13a** more energetic than **TS24a** (2.7 kcal mol^{-1}).

It is important to note that the domino reactions between **1** and **2** or **3** give two different outcomes: **1** + **2** gives the final cycloadducts **P1n** along mode B, whereas **P4a** is obtained from **1** + **3** along mode A. An analysis of the results can be done from the energy profiles depicted in Figure 5. For **1** + **2**, the [4 + 2] intramolecular cycloaddition along **TS24n** (mode A) is disfavored relative to the [4 + 2] intermolecular cycloaddition along **TS13n** (mode B), and the final cycloadduct **P1n** is obtained. However, for **1** + **3**, the [4 + 2] intramolecular cycloaddition along **TS24a** (mode A) is favored over the [4 + 2] intermolecular cycloaddition along **TS13a** (mode B), and consequently the final cycloadduct **P4a** with the two conjugated carboxylates is obtained. These different outcomes can be attributed to the fact that the formation of **P4n** along pathway A demands a conformational interconversion of **2a** to the more unfavorable syn arrangement, **2s**. This change increases the relative energies of **IN3n** and **TS24n** relative to **IN3a** and **TS21a**, 9.3 and 5.6 kcal mol^{-1}, respectively, making **TS24n** more unfavorable than **TS13n**. Moreover, as **2a** and **2s** are in conformational equilibrium, both conformers afford the final cycloadduct **P4n** via mode B. This fact opens the possibility that the Curtin−Hammett principle[26−28] can be operative in this domino reaction. These theoretical results are in agreement with the experimental data reported by Wynberg and Helder[9] and Wasserman and Kitzing[8] and allow us to explain the differing cycloadduct formation for these furanophanes systems.

The theoretical facts used to explain the experimental results prevail at the higher calculation level. Therefore, these results confirm Jursic's proposal[12−16] and justify the use of the B3LYP/6-31G*//AM1 approach for the study of large chemical systems that are of interest in synthetic organic chemistry. However, it is important to note that for the cycloaddition processes in these domino reactions, the PEBs calculated for the [4 + 2] intermolecular cycloaddition at the B3LYP/6-31G*//AM1 level present larger values than B3LYP/6-31G* calculations.

Conclusion

We have used AM1, B3LYP/6-31G*//AM1, and B3LYP/6-31G* approaches to investigate the PESs for the domino reactions of **1** with two furanophanes, **2** and **3**. The different reaction pathways have been mapped out, and TSs, intermediates, and final cycloadducts have been located and properly characterized. Within the limitations of the calculation levels, the results give a qualitative picture of these complex domino reactions. The theoretical results are in agreement with experimental outcome, and they are able to explain the origin of the chemical selectivity. We can conclude that the correct behavior of the systems under investigation is reproduced.

The present theoretical results point out that the different reactivity pattern is due to the different attack modes of DMAD to the furan ring or to the naphthalene/anthracene systems. For naphthalenofuranophane, the most favorable reaction pathway takes place along the initial [4 + 2] intermolecular cycloaddition involving the naphthalene system to give a benzobicyclo[2.2.2]octadiene intermediate (mode B), which by a subsequent [4 + 2] intramolecular cycloaddition gives the final product. For anthracenofuranophane, the most favorable reaction pathway takes place along an initial [4 + 2] intermolecular cycloaddition with participation of the furan ring to give an oxabicyclo[2.2.1]heptadiene intermediate

(26) Curtin, D. Y. *Recl. Chem. Prog.* **1954**, *14*, 111.

(27) Hammett, L. P. *Physical Organic Chemistry*; McGraw-Hill: New York, 1970.

(28) Seeman, J. I. *Chem. Rev.* **1983**, *83*, 83.

(mode A), which by a [4 + 2] intramolecular cycloaddition involving the nonsubtituted double bond affords the final cycloadduct.

These theoretical results are consistent with experimental investigations and shed light on the molecular mechanisms for other domino transformations, underlining the role played by the different energetic contributions along the reaction pathways for the formation of the different adducts.

Acknowledgment. This work was supported by research funds provided by the Conselleria de Cultura Educació i Ciéncia, Generalitat Valenciana (Project GV97-CB-11-86). M.O. thanks Ministerio de Educación y Ciencia (Spanish Goverment) for a fellowship. All AM1 calculations were performed on an O2 Silicon Graphics workstation of the Departamento de Química Orgánica of the Universidad de Valencia, and DFT calculations were performed on a Cray-Silicon Graphics Origin 2000 with 64 processors of the Servicio de Informática de la Universidad de Valencia. We are most indebted to this center for providing us with computer capabilities.

JO981442K